

行政院國家科學委員會補助專題研究計畫 ■ 期中進度報告

介觀結構的失相、暫態反應、量子傳輸等特性的研究(2/3)

A study on the dephasing, transient response, and quantum transport characteristics in mesoscopic structures

計畫類別： 個別型計畫  整合型計畫

計畫編號：NSC 91-2112-M-009-014-

執行期間： 91年8月1日 至 92年7月31日

計畫主持人： 朱仲夏

計畫參與人員： 唐志雄 國科會理論中心

A.G. Mal'shukov Institute of Spectroscopy, Russian  
Academy of Science

鐘淑維 國立交通大學電子工程系

王律堯 國立交通大學電子物理系

K.A.Chao Lund University

成果報告類型(依經費核定清單規定繳交)： 精簡報告  完整報告

本成果報告包括以下應繳交之附件：

赴國外出差或研習心得報告一份

赴大陸地區出差或研習心得報告一份

出席國際學術會議心得報告及發表之論文各一份

國際合作研究計畫國外研究報告書一份

處理方式：除產學合作研究計畫、提升產業技術及人才培育研究計畫、  
列管計畫及下列情形者外，得立即公開查詢

涉及專利或其他智慧財產權， 一年 二年後可公開查詢

執行單位：國立交通大學電子物理系

## 一、中文摘要

我們探討了介觀結構中三個時變量子傳輸的問題。

首先，我們提出了一個非絕熱量子抽運機制的實驗結構，並計算此結構的抽運特性，也仔細的研究其中的抽運機制，預測抽運電流是在奈安培的範圍。此實驗結構的特色，是只需控制一個相位差就能改變抽運電流的方向，另外，指狀閘極只需四個就能產生奈安培級的抽運電流。此部份的結果已分析完成，並已投稿至 Physical Review B.

其次，我們探討了利用時變偏壓的閘極在 Rashba spin-orbit 效應明顯的異質介面上所產生的交流自旋流。在 diffusive 的情況下，我們預測此等時變偏壓閘極的方式，能產生奈安培級的交流自旋流，我們也提出利用電閘極量測自旋流的機制。此部份的結果已分析完成(Cond-mat/0211559)，並已投稿。在 ballistic 的情況下，我們已完成理論推導以及 ballistic 窄通道在 Rashba spin-orbit 效應下電子態的計算與物理分析，此部份的結果已再 2003 年中華民國物理年會中報告，電子散射的數值計算與分析正在進行中。

第三，奈米結構在交流偏電壓閘極的作用下，除了產生抽運電流，熱流也是一個很重要的議題。我們計算了在這情形下的熱流特性，初步的結果是抽運電流與熱流有很密切的關係。

**關鍵詞：**量子傳輸，量子抽運，非絕熱，指狀閘極，自旋軌道作用，Rashba 項，自旋流的產生，相位差。

### Abstract

We have investigated three quantum transport problems in mesoscopic structures that involve time-modulated effects.

First, we have proposed an experimental configuration for the observation of a nonadiabatic quantum pumping mechanism. The mechanism is the time-dependent Bragg reflection, proposed also by us recently. We have also studied various quantum pumping characteristics of the proposed experimental configuration, and have analyzed in detail the connection of those characteristics with the nonadiabatic quantum pumping mechanism. The proposed experimental configuration has the advantage that the pumped current, and its direction, can be controlled by the tuning of only one phase difference. The pumped current is predicted to be of order nano-Ampere. We have finished our analysis and have submitted to Physical Review B.

Second, we have investigated the effect of an ac biased metal gate to the generation of spin current in the heterostructure of low energy gap semiconductor, such as InAs-InAlAs heterostructures, in which the Rashba spin-orbit interaction is important. In the diffusive regime, we have predicted that the ac biased gate can give rise to spin current of order nano-ampere. We have also proposed a non-magnetic and non-optical means of probing spin-current by the use of a metal gate. We have finished our analysis (Cond-mat/0211559), have presented in the 2003 American Physical Society March Meeting, and have submitted to be referred for publication. On the other hand, in the ballistic regime, we have finished the formulation and have analyzed the electron structures of a narrow channel in the presence of Rashba spin-orbit interaction. This part has been presented in the 2003 R.O.C. Physical Society Annual meeting. Further numerical work and the analysis for the electron scattering is currently being carrying out in its final stage.

Third, we have studied the heat current in a mesoscopic structure acted upon by ac biased

metal gates. Our preliminary result shows strong correlation between the pumped current and the heat current.

**Keywords:** quantum transport, quantum pumping, non-adiabatic, time-dependent Bragg reflection, finger gates, spin-orbit scattering, Rashba term, spin-current generation, phase difference.

## Gate-induced nonadiabatic quantum pumping

S. W. Chung<sup>1</sup>, C. S. Tang<sup>2</sup>, C. S. Chu<sup>3</sup>, and C.Y. Chang<sup>1</sup>

<sup>1</sup>*Department of Electronics, National Chiao-Tung University, Hsinchu 30050, Taiwan*

<sup>2</sup>*National Center for Theoretical Sciences, National Tsing-Hua University, Hsinchu 30050, Taiwan*

<sup>3</sup>*Department of Electrophysics, National Chiao-Tung University, Hsinchu 30050, Taiwan*

(Dated: June 1, 2003)

We propose an experimental configuration for nonadiabatic quantum pumping in a narrow constriction. Various pumping characteristics are demonstrated. The pumping potential is generated by ac biasing a pair of finger gate arrays (FGA). Pumping of charges is caused both by the mechanism of time-dependent Bragg reflections, and by the breaking of the electron transmission symmetry when the pumping potential is predominately of a propagating type. This propagating wave condition can be achieved by monitoring a phase difference  $\phi$  between the two FGAs.

Quantum charge pumping (QCP) has become an active field in recent years. This is concerned with the generation of net transport of charges across an unbiased mesoscopic structure by cyclic deformations of two structure parameters. Original proposal of QCP, in the adiabatic regime, is due to Thouless.<sup>1</sup> He considered the current generated by a slowly varying traveling wave that has both spatial and temporal periodicity. The adiabatic quantum pumping (AQP) problem was later cast into an elegant form by Brouwer.<sup>2</sup> An experimental confirmation of AQP was reported by Switkes *et al.*<sup>3</sup> Two metal gates that define the shape of an open quantum dot were biased with voltages of the same frequency but differ by a tunable phase difference. DC response across the source and drain electrodes is the signature of the AQP. This has prompted recent intensive studies on various aspects of AQP.<sup>4-11</sup>

An alternate experimental effort in generating QCP involves surface acoustic wave (SAW).<sup>12</sup> Generated by an interdigitated SAW transducer located deep in an end-region of a narrow channel, the SAW propagates to the other end-region of the narrow channel while inducing a wave of electrostatic potential inside the channel. Electrons trapped in the potential minima are thus transported along the narrow channel. Both Mott-Hubbard electron-electron repulsion in each such trap and the adiabaticity in the transport are needed to give rise to quantization in the pumped current.<sup>12</sup> As such, the channel was operated in the pinch-off regime.

In this work, we propose yet another experimental configuration for QCP. The pumping mechanism involved, however, is nonadiabatic in nature, and the channel is not in the pinch-off regime. A pair of FGA is used for the generation of pumping potential in a narrow channel. Rather than locating at a far distance away from the narrow channel, the FGA pair sits on top of it. The finger gates orient transversely and line up longitudinally with respect to the narrow constriction. As is shown in Fig. 1, the FGA pair is ac biased with the same frequency but a phase difference  $\phi$  is maintained between the FGA pair. Since the wave of electrostatic potential induced in the narrow channel is directly from the finger gates, rather than via the SAW, our proposed structure has the

obvious advantage that the working frequency is not restricted to the frequency of the SAW,  $\omega_{\text{SAW}} = 2\pi v_{\text{SAW}}/d$ . Here  $v_{\text{SAW}}$  is the phase velocity of the SAW, and  $d$  is the pitch in the FGA. Furthermore, when the working frequency is different from  $\omega_{\text{SAW}}$ , the contribution from SAW to the pumped current will be negligible.

More importantly, we show that the ac biased FGA pair plays a more subtle role in the generation of QCP. The FGA pair causes the traversing electron to undergo time-dependent Bragg reflection – the coherent inelastic scattering that resonantly couples the electron and photon. This resonant coupling breaks the transmission symmetry when the electrostatic potential has a preferred propagation direction. The proposed FGA pair provides a simple way of changing the preferred propagation direction by monitoring a phase difference  $\phi$ . That the contribution of this time-dependent Bragg reflection to QCP is robust is demonstrated by considering FGA that consists of only four finger gates. Our time-dependent scattering approach goes beyond adiabatic condition and is formally exact.<sup>13</sup>

The potential  $V(x, t)$  in the narrow constriction induced by a FGA pair is represented by

$$V(x, t) = \sum_{i=1}^N \{V_1 \delta(x - x_i) \cos(\Omega t) + V_2 \delta(x - x_i - \delta x) \cos(\Omega t + \phi)\}, \quad (1)$$

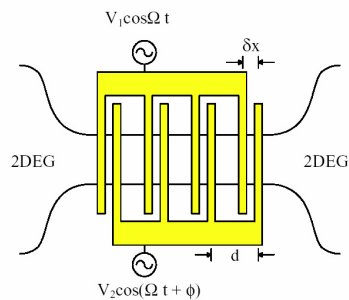


FIG. 1: Proposed system structure. A FGA pair locates on top of a narrow channel.  $\hat{V}$  denotes the amplitude of the potential energy, and  $\phi$  is the phase difference.

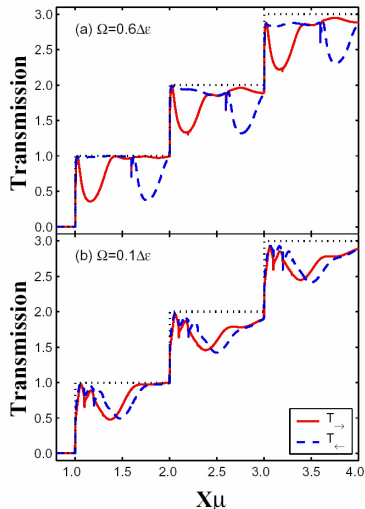


FIG. 2: Total current transmission coefficient versus  $X_\mu$  for (a)  $\Omega = 0.6\Delta\epsilon$ , and (b)  $\Omega = 0.1\Delta\epsilon$ . The transmission of the right-going (left-going) electrons are represented by the solid (dotted) curve. The subband level spacing is  $\Delta\epsilon$ . Parameters  $\alpha = 1/4$  and  $\phi = \pi/2$  are chosen to meet the optimal condition.

where  $N$  is the number of finger gates per FGA. These finger gates are evenly spaced, with a pitch  $d$ , and are located at  $x_i = (i-1)d$  for one FGA and  $x_i + \delta x$  for the other. The relative shift between the FGA pair is  $\delta x = \alpha d$ , where the fractional shift  $0 < \alpha < 1$ . In the following, we consider the case  $V_1 = V_2 = V_0$ . Depending on the choice of the values for  $\phi$  and  $\alpha$ ,  $V(x, t)$  will either be predominately of propagating or standing wave type. A sensible choice can be made from considering the lowest order Fourier component of  $V(x, t)$ , given by  $(2V_0/d)\{\cos Kx \cos \Omega t + \cos[K(x - \delta x)] \cos(\Omega t + \phi)\}$ , where  $K = \frac{2\pi}{d}$ . For our purposes in this work, an optimal choice will be  $\phi = \frac{\pi}{2}$  and  $\alpha = \frac{1}{4}$ , in which  $V(x, t)$  is predominately a left-going wave.

The Hamiltonian is  $H = H_y + H_x(t)$ , where  $H_y = -\frac{\partial^2}{\partial y^2} + \omega_y^2 y^2$  contains a transverse confinement, leading to subband energies  $\epsilon_n = (2n+1)\omega_y$ . The time-dependent part of the Hamiltonian  $H_x(t)$  is of the form  $H_x(t) = -\frac{\partial^2}{\partial x^2} + V(x, t)$ . Here appropriate units have been used such that all physical quantities presented are in dimensionless form.<sup>13</sup>

In the QCP regime, the chemical potential  $\mu$  is the same in all reservoirs. Thus the pumped current, at zero temperature, is equal to

$$I = -\frac{2e}{h} \int_0^\mu dE [T_{\rightarrow}(E) - T_{\leftarrow}(E)] \quad (2)$$

where the total current transmission coefficient  $T_{\rightarrow(\leftarrow)}(E) = \sum_n \sum_m T_{n\rightarrow(\leftarrow)}^m$  is summed over all

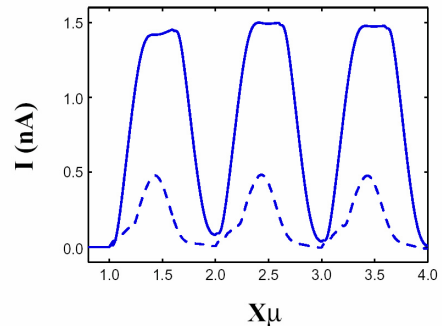


FIG. 3: Pumped current versus  $X_\mu$ . The choices of parameters are the same as in Fig. 2. The solid, and dashed, curves correspond, respectively, to  $\Omega = 0.6\Delta\epsilon$ , and  $\Omega = 0.1\Delta\epsilon$ .

the propagating components of the transmitted electrons, and includes both subband indice  $n$  and sideband indice  $m$ . The arrow in the total current transmission coefficient indicates the incident direction. The sideband indice  $m$  refers to the inelastic process that an electron with incident energy  $E$  emerges from the pumping region with energy  $E + m\Omega$ .

The unit scales in our numerical results are taken from the GaAs-Al<sub>x</sub>Ga<sub>1-x</sub>As heterostructure system. The values that we choose for our configuration parameters are  $\omega_y = 0.007$ , subband level spacing  $\Delta\epsilon = 2\omega_y$  ( $\simeq 0.13$  meV),  $d = 40$  ( $\simeq 0.32 \mu\text{m}$ ),  $N = 4$ , and  $V_0 = 0.04$  ( $\simeq 0.028$  meV  $\text{\AA}$ ). From the value of  $V_0$ , and the assumed finger gate width  $\sim 0.05 \mu\text{m}$ , the amplitude of the potential induced by a finger gate is  $\sim 0.056$  mV.

In Fig. 2, we present the dependence of the total current transmission coefficients on  $\mu$ . The chemical potential  $\mu$ , however, is replaced by  $X_\mu = \mu/\Delta\epsilon + \frac{1}{2}$ , which integral value corresponds to the number of propagating subbands in the narrow channel. The frequencies are (a)  $\Omega = 0.6\Delta\epsilon$  ( $\Omega/2\pi \simeq 18$  GHz), and (b)  $\Omega = 0.1\Delta\epsilon$  ( $\Omega/2\pi \simeq 3$  GHz). With the optimal choices of the parameters  $\phi$  and  $\alpha$ , the pumping potential  $V(x, t)$  is essentially a left-going wave.

At integral values of  $X_\mu$ , the total current transmission coefficients  $T_{\rightarrow(\leftarrow)}$  exhibit abrupt changes. This is due to the changes in the number of propagating subbands in the narrow channel. Between integral  $X_\mu$  values,  $T_{\rightarrow(\leftarrow)}$  show both valley and dip structures. These dip structures occur at, respectively,  $X_\mu = n + 0.6$  and  $X_\mu = n + 0.1, n + 0.2$  in Figs. 2(a) and (b); are the same for both  $T_{\rightarrow(\leftarrow)}$ ; and are resonances associated with inelastic scattering into a quasi-bound state (QBS) just beneath a subband bottom.<sup>14</sup> On the other hand, the valley structures occur at different  $X_\mu$  for  $T_{\rightarrow}$  and  $T_{\leftarrow}$ , with  $T_{\rightarrow}$ 's valley occurs at a lower  $X_\mu$ . This shows clearly the breaking of the transmission symmetry by the pumping potential. Furthermore, the valleys are separated by  $\Delta X_\mu = \Omega/\Delta\epsilon$ . This can be understood from a resonant coupling condi-

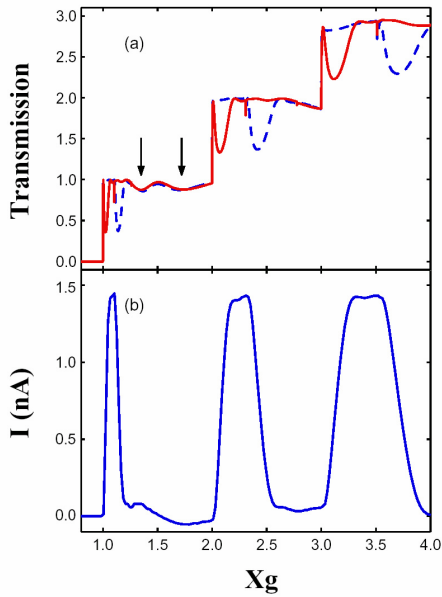


FIG. 4: The dependence on  $\omega_y$  of (a) the total current transmission coefficient, and (b) the pumped current. The abscissa is depicted by  $X_g = \mu/\Delta\epsilon + \frac{1}{2}$  where  $\mu = 0.049$  ( $X_\mu = 3.5$ ). Frequency  $\Omega = 0.0084$  in all curves except for the dotted curve in (b), where  $\Omega = 0.0014$ . Parameters  $\phi = \pi/2$  and  $\alpha = 0.25$  for all curves except for the dashed curve in (b), where  $\alpha = 0.2$ . In (a), the solid (dashed) curve is for  $T_+$  ( $T_-$ ), and contributions from the second Fourier component of  $V(x, t)$  are indicated by arrows.

tion  $\epsilon_k = \epsilon_{k-K} \mp \Omega$ ,<sup>13</sup> where the upper sign is for positive (right-going)  $k$ . From this condition, the valley locations can be determined, and are at  $k_{\pm}^2 = [(K/2)(1 \mp \Omega/K^2)]^2$ . These locations, given by  $X_\mu = k_{\pm}^2/\Delta\epsilon + n$ , are at  $X_\mu = 1.19, 1.79, 2.19, 2.79, 3.19$ , and  $3.79$  for the case of Fig. 2(a), and  $X_\mu = 1.39, 1.49, 2.39, 2.49, 3.39$ , and  $3.49$  for the case of Fig. 2(b). The matching between these numbers and our numerical results in Fig. 2 is remarkable. In addition, energy gaps open up at these  $k_{\pm}^2$  locations, causing the drop in the transmission and the formation of the valley structures. All these results reassure us that the aforementioned resonance condition, or equivalently, the time-dependent Bragg's reflection, is the dominant pumping mechanism in our FGA pair structure. The mechanism is nonadiabatic by nature.

In Fig. 3, we present the  $X_\mu$  dependence of the pumped current for the cases in Fig. 2. The pumped current peaks when  $X_\mu$  lies in between the valley structures in the total current transmission coefficients. The peaks have flat tops for the solid curve, when  $\Omega = 0.6\Delta\epsilon$ . Comparing with the total current transmission curves in Fig. 2(a), we see that the flat-topped peak in the pumped current is associated with the situation when the valleys in  $T_+$  and  $T_-$  are completely cleared from one another. For

the case when the valleys overlap, such as in Fig. 2(b), the pumped current peaks are no longer flattened, as is shown by the dashed curve in Fig. 3. However, their peak values are lowered. It is also of interest to note that the pumped currents are of order  $n\text{Å}$ . This demonstrates the robustness of the pumping effect in our proposed FGA pair. It is also worth pointing out that the pumped currents are positive in Fig. 3, showing that the net number flux of the pumped electrons is from right to left. This is consistent with the propagation direction of the electrostatic wave in  $V(x, t)$ .

Thus far, we have explored the dependence of the FGA pair's QCP characteristics on  $X_\mu$ , or equivalently, on the electron density in the system. This can be realized experimentally by the use of the back-gate technique. Modulation of the width of the narrow channel is another mode of tuning the QCP characteristics. This can be realized experimentally by the use of the split-gate technique. Hence we present, in Fig. 4, the transverse confinement dependence of both the total current transmission coefficients and the pumped current. The transverse confinement is depicted by  $X_g = \mu/\Delta\epsilon + \frac{1}{2}$ , which relation to the effective channel width is linear, and that, again, its integral value corresponds to the number of propagating subbands in the channel. In this mode of tuning the QCP characteristics,  $\mu$  is kept fixed.

In Fig. 4(a), except for  $\mu$ , which is fixed at 0.049, and  $\omega_y$ , other parameters such as  $\Omega = 0.0084$ ,  $\phi = \pi/2$ , and  $\alpha = 0.25$  are the same as in Fig. 2(a). The solid (dashed) curve is for  $T_+$  ( $T_-$ ). Both the QBS and the time-dependent Bragg reflection features are found. The expected locations of the QBS, given by the expression  $X_g = \frac{1}{2} + (n + \frac{1}{2})\mu/(\mu - \Omega)$ , should be at 1.1, 2.3, and 3.5, and they matches the QBS locations perfectly. The expected locations of the valleys, associated with the time-dependent Bragg reflection, are given by the expression  $X_g = \frac{1}{2} + (n + \frac{1}{2})\mu/(\mu - k_{\pm}^2)$  and they should be at 1.03, 2.1, 3.14 for  $T_+$ , and at 1.15, 2.4, 3.73 for  $T_-$ . Again, the matches with the valley locations are remarkable.

Besides, there are in Fig. 4(a) two additional valley structures, indicated by arrows, at which  $T_+$  and  $T_-$  almost fall one on top of the other. These structures do not contribute to the pumped current. Furthermore, these structures are due to the time-dependent Bragg reflection from the second order Fourier component of  $V(x, t)$ . From the resonant coupling condition  $\epsilon_k = \epsilon_{k-2K} \mp \Omega$ , the valley locations should be at  $\frac{1}{2}[1 + \mu/(\mu - \epsilon_{\pm})]$  for  $n = 0$ , where the upper sign is for positive (right-going)  $k$ , and  $\epsilon_{\pm} = [K(1 \mp \Omega/(2K)^2)]^2$ . Thus the valley locations are expected to be at 1.36 and 1.73, which coincide with the two additional valleys in Fig. 4(a). In addition, the second Fourier component of  $V(x, t)$  is in the form of a standing wave,  $\cos(2Kx)[\cos\Omega t + \sin\Omega t]$ . This explains why that the two valleys appear in both  $T_+$  and  $T_-$ . We note also that the contribution from the higher Fourier components drop quite rapidly, as is seen by comparing the valleys from the first and the second Fourier components of  $V(x, t)$ .

The  $X_g$  dependence of the pumped current for the case in Fig. 4(a) is represented by the solid curve in Fig. 4(b). The peaks have flat tops because the valleys in the corresponding  $T_{\rightarrow}$ ,  $T_{\leftarrow}$  are well separated. The pumped current for  $\Omega = 0.0014$ , the same frequency as in the case of Fig. 2(b), is depicted by the dotted curve in Fig. 4(b). The peaks are not flat-topped and the magnitudes are much smaller because the transmission valleys overlap. For comparison, we also present the case when the optimal choices has not been made. As is shown by the dashed curve in Fig. 4(b), where all parameters are the same as in the solid curve except that  $\alpha = 0.2$  rather than 0.25, the basic pumped current peaks remain intact while additional pumped current peaks can be shown to arise from the second Fourier component of  $V(x, t)$ . This also demonstrates the robustness of the QCP against the

deviation from the optimal choice of the configuration parameters.

In conclusion, we have proposed a finger-gate array pair configuration for the generation of quantum charge pumping. The pumping characteristics have been investigated and the pumping mechanism understood.

#### Acknowledgments

The authors wish to acknowledge the National Science Council of the Republic of China for financially supporting this research under Grant Nos. NSC91-2112-M-009-014, and NSC90(91)-2119-M-007-004(NCTS).

- 
- <sup>1</sup> D.J. Thouless, Phys. Rev. B **27**, 6083 (1983).  
<sup>2</sup> P.W. Brouwer, Phys. Rev. B **58**, R10135 (1998).  
<sup>3</sup> M. Switkes, C.M. Marcus, K. Campman, and A.C. Gosard, Science **283**, 1905 (1999).  
<sup>4</sup> F. Zhou, B. Spivak, and B. Altshuler, Phys. Rev. Lett. **82**, 608 (1999).  
<sup>5</sup> Yadong Wei, Jian Wang, and Hong Guo, Phys. Rev. B **62**, 9947 (2000).  
<sup>6</sup> M.L. Polianski and P.W. Brouwer, Phys. Rev. B **64**, 75304 (2001).  
<sup>7</sup> J.E. Avron, A. Elgart, G.M. Graf, and L. Sadun, Phys. Rev. Lett. **87**, 236601 (2001).  
<sup>8</sup> M. Moskalets and M. Büttiker, Phys. Rev. B **64**, 201305 (2001).  
<sup>9</sup> M. Moskatlets and M. Büttiker, Phys. Rev. B **66**, 035306 (2002).  
<sup>10</sup> O. Entin-Wohlman and Amnon Aharony, Phys. Rev. B **66**, 035329 (2002).  
<sup>11</sup> Baigeng Wang, and Jian Wang, Phys. Rev. B **66**, 125310 (2002).  
<sup>12</sup> V.I. Talyanskii, J.M. Shilton, M. Pepper, C.G. Smith, C.J.B. Ford, E.H. Linfield, D.A. Ritchie, and G.A.C. Jones, Phys. Rev. B **56**, 15180 (1997); J.M. Shilton, V.I. Talyanskii, M. Pepper, D.A. Ritchie, J.E.F. Frost, C.J.B. Ford, C.G. Smith, and G.A.C. Jones, J. Phys.: Condens. Matter **8**, L531 (1996); J.M. Shilton, D.R. Mace, V.I. Talyanskii, Yu. Galperin, M. Y. Simmons, M. Pepper, and D.A. Ritchie, J. Phys.: Condens. Matter **8**, L337 (1996).  
<sup>13</sup> C.S. Tang and C.S. Chu, Solid State Commun. **120**, 353 (2001).  
<sup>14</sup> P.F. Bagwell and R.K. Lake, Phys. Rev. B **46**, 15329 (1992), C.S. Tang and C.S. Chu, Phys. Rev. B **53**, 4838 (1996).

***Conference papers:***

**The 2003 annual meeting of the Physical Society of the Republic of China**

Effect of Rashba mechanism on transport characteristics in a narrow channel

L. Y. Wang<sup>a</sup>, J. Y. Chiu<sup>a</sup>, Y. Y. Lin<sup>a</sup>, C. S. Tang<sup>b</sup>, C. S. Chu<sup>a</sup>

<sup>a</sup>Department of Electrophysics, National Chiao Tung University

<sup>b</sup>National Center for Theoretical Sciences, National Tsing Hua University

(Oral presentation)

Nonadiabatic quantum pumping in a narrow constriction

S.W. Chung<sup>a</sup>, C.S. Tang<sup>b</sup>, C.S. Chu<sup>c</sup>

<sup>a</sup>Dept. of Electronic Engineering, National Chiao Tung University

<sup>b</sup>National Center for Theoretical Sciences, National Tsing Hua University

<sup>c</sup>Department of Electrophysics, National Chiao Tung University

**2003 APS March Meeting**

Spin current generation and detection in the presence of AC gate

C.S. Chu<sup>a</sup>, A.G. Mal'shukov<sup>b</sup>, C.S. Tang<sup>c</sup>, and K.A. Chao<sup>d</sup>

<sup>a</sup>Department of Electrophysics, National Chiao Tung University, Hsinchu, Taiwan, R.O.C.

<sup>b</sup>Institute of Spectroscopy, Russian Academy of Science, Troitsk, Moscow, Russia

<sup>c</sup>National Center for Theoretical Sciences, Hsinchu, Taiwan, R.O.C.

<sup>d</sup>Solid State Theory Division, Department of Physics, Lund University, Sweden

D29.14

Nonadiabatic quantum pumping in a narrow constriction

C.S. Tang<sup>a</sup>, S.W. Chung<sup>b</sup>, C.S. Chu<sup>c</sup>

<sup>a</sup> National Center for Theoretical Sciences, Hsinchu, Taiwan, R.O.C.

<sup>b</sup> Dept. of Electronic Engineering, National Chiao Tung University, Hsinchu, Taiwan, R.O.C.

<sup>c</sup>Department of Electrophysics, National Chiao Tung University, Hsinchu, Taiwan, R.O.C.

B22.10

***Paper published:***

C.S. Tang, Y.H. Tan, and C.S. Chu

“Transport spectroscopy in a time-modulated open quantum dot”

Physical Review B **67**, 205324 (2003)

***Paper submitted:***

A.G. Mal'shukov, C.S. Tang, C.S. Chu, and K.A. Chao

“Spin-current generation and detection in the presence of ac gate”



submitted to Physical Review Letter.

(see also Cond-mat/0211559)

S.W. Chung, C.S. Tang, C.S. Chu, and C.Y. Chang

“Gate-induced nonadiabatic quantum pumping”

submitted to Physical Review B.